RSC Advances

ROYAL SOCIETY OF CHEMISTRY

www.rsc.org/advances

Chiral segregation of hockey-stick shaped particles in two dimensions

J. A. Martínez-González,[a‡] R. Pablo-Pedro,[ax] J.C. Armas-Pérez,[c¶] G. A. Chapela[b] and J. Quintana-H[* a]

Received Xth XXXXXXXXXX 20XX, Accepted Xth XXXXXXXXX 20XX
First published on the web Xth XXXXXXXXXX 200X
DOI: 10.1039/b000000x

Chiral segregation and liquid crystalline aggregates in two dimensions are studied for a heterochiral mixture of an oversimplified version of the so called Hockey Stick-shaped particles, made with two line segments that interact via an infinitely repulsive potential. The goal of this study was to explore the possibility to produce chiral segregation and to find the liquid crystalline mesophases using this model which has an extreme level of idealization. This is, considering infinitely thin particles, infinite repulsions interacting side-side exclusively, namely, the substrate does not act on the molecules. Since only infinite repulsions are considered, the phase behavior is ruled by entropic effects, where self-assembly takes place. Onsager theory and Monte Carlo simulations in the Gibbs and the canonical ensembles were used to study several molecular conformations in order to delineate the mesophases diagram which includes the chiral segregation region and several liquid crystalline mesophases, most of them are heterochiral. The enantiomerically pure phase is of the smectic kind and corresponds to the highest density regime. The heterochiral mesophases are nematic, smectic with antiferroelectric order and tetratic. The appearance of the different assemblies strongly depend on the molecular conformation defined by the angle between the segments and their lengths. To study the phase transitions, the molar concentration, the nematic and tetratic order parameters, as well as the distribution functions were calculated.

1 Introduction

Chirality is a phenomenon where symmetry plays an essential role. It has important consequences in several fields of natural sciences like chemistry, biology and physics. Chirality at molecular level, gives rise to a pair of mirror-image molecules, called enantiomers. Although the similarities in the enantiomeric pair components, such as identical physical or chemical properties, each of them may have very different or even opposite effects in alive beings. This is the reason why the separation of enantiomeric mixtures is of fundamental interest in the food and pharmaceutical industry. At the same time, the presence of chirality in material science may change the characteristics of materials opening diverse possibilities for their fabrication.

In nature, the production of chiral components is asymmetrical, this is, components of alive beings, such as amino acids or sugars, have a specific chirality. On the other hand, in the laboratory synthesis of chiral compounds produce heterochiral mixtures, unless special procedures are applied[1].

Spontaneous separation of racemic mixtures (50% of each component) is not frequent, only less than approximately 10% have been reported[2]. The first one was discovered by Pasteur using a crystallization process in the bulk. However in the laboratory, unless special procedures are applied, synthesis of chiral compounds results in a racemic mixtures[1]. In recent years, several experiments have shown that enantiomeric separation can be enhanced in situations that show some kind of constraints. For example, to reduce the dimensionality of the system, creating a reduction of the spatial degrees of freedom and therefore a change of the symmetry rules. One of the consequences of this is that there are systems that in three dimensions are not chiral but when they are confined to a bi-dimensional domain the structure can be considered chiral. Molecules with this feature are called pro-chiral[3] and the molecular model considered in this paper is one example. Another characteristic that seems necessary is that this phenomenon occurs at high density regimes. For example the molecular self assembling that occurs in two dimensional domains[4]. One of the earliest experiments that have been reported is the spontaneous chiral separation of amphiphilic

[a] *Instituto de Química, Universidad Nacional Autónoma de México - Apdo. Postal 70213, 04510, Coyoacán, México D.F., México. Fax:, Tel: +52 55 56224510; E-mail: jaq@unam.mx*
[b] *Departamento de Física, División de Ciencias Básicas, Universidad Autónoma Metropolitana, Iztapalapa, México D.F., México.*
‡ Present address: Departamento de Física, División de Ciencias Básicas, Universidad Autónoma Metropolitana, Iztapalapa, México D.F., México.
§ Present address: Department of Chemistry, Massachusetts Institute of Technology, 77 Massachusetts avenue , Cambridge, Massachusetts 02139, USA.
¶ Present address: Institute for Molecular Engineering, University of Chicago, Chicago, Illinois 60637, USA.

molecules in a monolayer by Nassoy et al[4] in a Langmuir balance. Chiral domains of small size are formed by reduction of the surface of the monolayer formed in the water-air interface. Some other experiments have been performed using the Langmuir-Blodgett device where also chiral segregation occurs[5]. In these cases, the substrate is a central part in the separation process. In general in all those experiments, the common characteristic is that considerable degree of molecular ordering, positional and orientational is present. However, Huang et al.[6] found that the orientation may not be necessary.

Important efforts have been done in order to elucidate this complex phenomenon. From the theoretical point of view, Huckaby et al. was one of the pioneers to attack this problem using lattice models. Since the decade of the 80's they published several papers where the particles used were adsorbed onto a plane[7,8]. More recently, they studied the chiral separation of the Andelman de Gennes[9] model using different kinds of interactions, including van der Waals and electrostatics[10]. From simulations there are also several studies on this topic[11,12]. Despite the fact that there have been several attempts dedicated to analyze this problem, the understanding of the molecular details that enhance the chiral separation is still incomplete.

The background behind this paper is that a similar system, constructed by three segments, the zigzag model, interacting with infinitely repulsive potentials and confined to a 2D domain was able to show chiral separation[13]. In this case, since the system was athermal, the phase separation was ruled only by the density. Complementary studies of the zigzag model, were devoted to investigate its liquid crystalline behavior. The first, using Monte Carlo isobaric ensemble[14] and then applying the Onsager theory[15,16].

The general goal of this paper is to investigate the ability to produce chiral phase separation considering a modification of the zigzag system where the present model has only two segments. This over simplified system, built with only two lines, is called the Hockey-Stick shaped particle[17]. The molecular conformations used for this paper are those that create chiral structures, i.e. where the the length of the two segments are unequal.

The paper is organized as follows, Introduction is found in section 1, the definition of the model and the simulation details are in section 2, section 3 contains the Results and their explanations and finally the Conclusions are in section 4.

2 The Model and Monte Carlo Simulations Details

A two-dimensional hard body model whose shape mimics the Hockey-Stick (HSM) molecules is studied. Our model particle consists of two line segments of unequal length. The lengths of the segments are a and b, i.e. the total length of the model particle is $L = a + b$. The model is sketched in Fig. 1.

Our previous study[17] has been extended by examining the chiral segregation in HSM with $a = 0.11$, 0.15, 0.18, 0.20, 0.22, 0.25, 0.30, 0.35, 0.40 and 0.45, for $\theta = \pi/4$ and $\pi/2$. Note that the total length of the particle is $L = 1$, i.e. $b = 1 - a$. The total number of particles in the simulation was $N = 1000$.

Fig. 1 Hard body representation of a HSM molecule consisting of two line segments with $a + b = L = 1$ and a bend angle θ between them. The arrow does not belong to the particle, it represents the polar axis of the particle.

The density is defined as $\rho^* = N/(L_x^* * L_y^*)$ where L_x^* and L_y^* are the simulation box lengths for x and y axes respectively and L is used to make the lengths dimensionless $r* = r/L$. The dimensionless pressure is defined as $p^* = p\beta L^2$ where $\beta = 1/k_BT$ and k_B is the Boltzmann constant and T is the temperature. Because the model is athermal the temperature has been set to $k_BT = 1$.

For chiral segregation studies, Monte Carlo simulations in the Gibbs ensemble (GEMC) were performed. The use of this ensemble allows the simulation of the phase coexistence of two enantiomerically different phases. Despite the chiral separation process is reached at high densities, it is possible to use the Gibbs ensemble because of the thickness of the model considered. According to the standard methodology[18], three types of configurational changes were performed: (a) random displacements or orientation changes were performed for randomly selected particles (b) changes in the area of the simulation boxes and (c) randomly selected particles were transferred from one of the simulation boxes to the other. In this work a Monte-Carlo cycle (MCC) consisted of 10000 attempts of displacements or orientation changes, 1 attempt of area change and about 1000 attempts of particle swaps. Approximately 4×10^6 MCC were required for equilibration and other 2×10^6 MCC to obtain statistics.

The acceptance criterion for these trial moves corresponds to the standard Metropolis algorithm for this ensemble. The maximum displacement, rotation angle and area change was adjusted during the simulation so that roughly 30% of these types of moves are accepted. The number of particles in each box at the beginning of the simulations was 500. In order to verify the lack of influence of the initial configuration in our results, we performed simulations were the initial composition of the two regions was either heterochiral or fully segregated (pure phases of each enantiomer in each region, see section 3).

Finally, the order parameter that characterizes the phase transition that produces chiral separation is the configurational

average of the molar fractions X_S and X_R of the simulation boxes, where the subscripts refer to right (R) and left (S) enantiomers. The criterion adopted is as follows,[19] segregation is considered finished when in one of the boxes the molar fractions $X_S \geq 0.85$ and $X_R \leq 0.15$, while in the other box the opposite occurs.

The orientational order in the mesophases was quantified by means of the order parameter given by $S_m = \max < \cos[m(\phi - \phi_0)] >$, where ϕ is the angle between the molecular axis of the particle and the axis of reference and ϕ_0 defines the vector $\mathbf{n} = (\cos\phi_0, \sin\phi_0)$ which provides the natural coordinate system for orientationally ordered phases. When $m = 2$, S_m gives the nematic order parameter, while $m = 4$ provides the tetratic order parameter. Similarly, for nematic and tetratic order, the orientational correlation function is $g_m(r^*) =< \cos m(\phi - \phi_0) >_r$, where the average is taken over a pair of particles.

Several studies in 2D indicate that the nematic and tetratic order parameters vanish in the thermodynamic limit and the orientational correlation functions g_2 and g_4 have a power law decay, which are indications of a quasi-long range order (QLRO) for both mesophases[17,20–23]. Because of the fact that g_2 and g_4 have an exponentional decay in the isotropic phase, the change in their behavior is a consequence of a phase transition.

Canonical simulations were implemented to complement GEMC simulations. In particular to compute the nematic (S_2) and tetratic (S_4) order parameters, as well as the radial correlation function ($g(r^*)$) and the orientational correlation functions ($g_2(r^*)$ and $g_4(r^*)$).

3 Results

Since the model is athermal, the only thermodynamic variable that rules the phase transitions is the density ρ^*. The Gibbs ensemble was simulated using a wide range of densities, several molecular conformations $a = 0.1, 0.15, 0.2, 0.25, 0.3, 0.4$, and using two molecular angles $\theta = \pi/2, \pi/4$. In all cases, the initial configuration was heterochiral (racemic) for both boxes. For sufficiently low densities, the isotropic structure was obtained. As the density was raised, orientational correlations start to appear, more explicitly, for enough anisotropic molecular conformations.

For $\theta = \pi/2$, the hetrochiral nematic N was developed for $a \leq 0.15$, while for $0.15 \leq a \leq 0.225$ the heterochiral tetratic T was displayed for $\rho^* \approx 20$ (see Fig. 2 b). The S_2 and S_4 order parameters for different a-values as well as the orientational correlation functions g_2 and g_4 for $a = 0.11$ and $a = 0.20$ are plotted in Fig. 3 where the change of decay for different values density can be appreciated. As can be observed, the nematic order parameter S_2 is reported for $a = 0.11, 0.15$, while for the other values of a the tetratic order parameter S_4 is shown. Only for $a = 0.15$, the system presents I-T, T-N and N-Sm phase transitions.

The positional correlations were developed for sufficiently high densities that depend on the molecular anisotropy. For example, for $a > 0.25$ a racemic smectic order SmR is obtained, this structure is globally heterochiral in both boxes (see Fig. 2c). In this kind of smectic order the rows have both kinds of enantiomers which are alternating each other producing heterochiral rows. Chiral segregation was obtained as two homochiral smectic phases coexisting, each one, in a simulation box (see Fig. 2 d). It should be noted that both phases are chiral and it is represented by the asterisk in the notation (Sm*). For $a \leq 0.25$ chiral separation is a result of a nematic-smectic phase transition, while for $a > 0.25$ it is a consequence of a smectic-smectic phase transition, from a heterochiral smectic to a homochiral smectic. In all cases the specific value of density depends on the molecular conformation. A qualitative mesophases diagram is shown in Fig. 4.

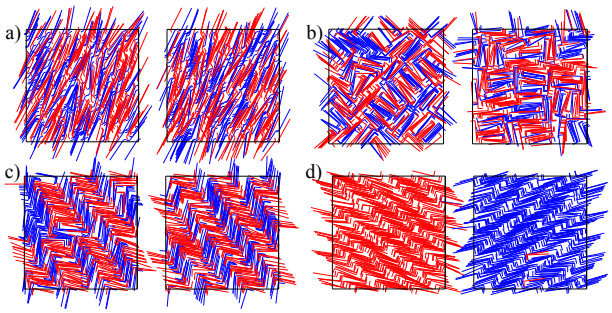

Fig. 2 Representative snapshots of the obtained configurations by Gibbs ensemble. a) N, $a = 0.11$, $\rho^* = 30$ and $\theta = \pi/4$, b) T, $a = 0.18$, $\rho^* = 25$ and $\theta = \pi/2$, c) SmR, $a = 0.25$, $\rho^* = 30$ and $\theta = \pi/2$, d) Sm* (segregation), $a = 0.20$, $\rho^* = 30$ and $\theta = \pi/2$

.

For $\theta = \pi/4$, a tetratic order was not observed and higher densities were required to get chiral segregation as can be appreciated in Fig. 4. Fig. 5 shows a comparison of the lowest densities for which segregation was obtained as a function of the parameter a of the model. It is possible to appreciate from the figure that $a = 0.25$ is the value that favors chiral segregation for both bent angles, and when $a \to 0.5$ or $a \to 0$ the density increases dramatically. Actually, chirality is lost in the banana limit ($a = 0.5$) and in the hard needles limit ($a = 0$), where the simulation results coincide with those previously reported for these cases[20,23]. The difference with the homochiral case[17,20] is that in heterochiral systems of HSM molecules there is a tetratic behavior for $\theta = \pi/2$, and because of the effect of the excluded area between enantiomeric pairs, the smectic phase is obtained for higher densities in both cases ($\theta = \pi/2$ and $\theta = \pi/4$).

As mentioned, this model shows isotropic (I), nematic (N),

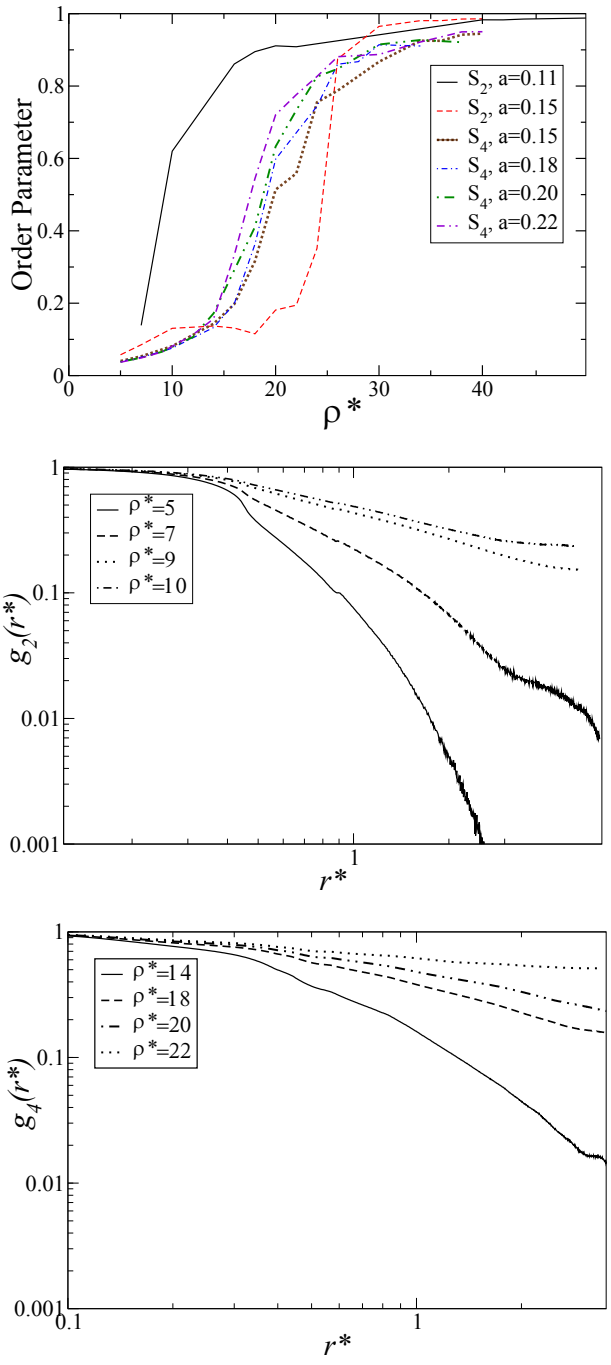

Fig. 3 (Color online) Nematic and tetratic order parameters (top), and the orientational correlation functions in log-log scale g_2 and g_4 for $a = 0.11$ and $a = 0.20$ respectively.

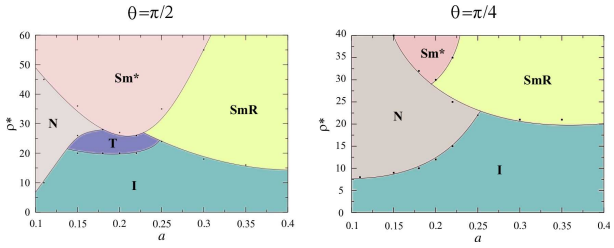

Fig. 4 Mesophases diagram, density as a function of the molecular parameter a, for a) $\theta = \pi/2$ and b) $\theta = \pi/4$, the dots are the simulation results and the lines are just to guide the eye.

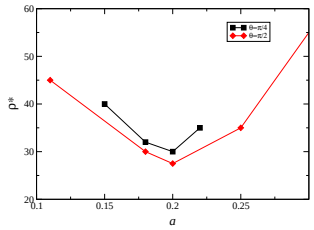

Fig. 5 The graph shows the lowest density in the simulations for which the system segregates as a function of the molecular parameter a.

heterochiral-smectic (SmR) and tetratic behavior, this last one for $\theta = \pi/2$, and the chiral segregation is given in two chiral smectic phases (Sm*), actually these smectics have an antiferroelectric order.

It is possible to explain the formation of all these structures by means of the second virial theory which has been successfully used to study the isotropic-nematic and the nematic-smectic phase transitions of banana and hockey-stick particles in two dimensions,[16,17,20]. In this work we focused in showing what kind of smectic correlations (Sm* or SmR) are more favorable according to the values of a, θ and ρ^*.

Because of the fact that we considered only hard interactions, the formation of mesophases is ruled by the entropic effects which are related with the excluded area. Based on the second virial theory the free energy F can be written as the sum of an ideal energy F_{id} and an excess contribution F_{ex},

$$\frac{\beta F}{A} = \frac{\beta F_{\mathrm{id}}}{A} + \frac{\beta F_{\mathrm{ex}}}{A}, \qquad (1)$$

where A is the total area.

In processes where the density is continuously increased and the system shows a N-Sm* phase transition, just before the smectic phase is formed, the nematic phase is orientationally well ordered. As a result in the study of the N-Sm* phase transition it is possible to assume the nematic phase as formed by a mixture of perfectly aligned particles. The "species" of this mixture are the possible orientations of the particles and they are referred to as conformations. In the case of a nematic

phase made by one component with polar geometry, there are two conformations (up and down), while in the case of two components (as it happens in the heterochiral mixture) there are four conformations (each component can be up or down, see Fig. 6 a). Therefore the ideal and the excess contributions of the free energy are given by,

$$\frac{\beta F_{\rm id}}{A} = \frac{1}{d}\sum_i \int_0^d \{\rho_i(y)\ln\rho_i(y) - \rho_i(y)\}\,{\rm d}y, \qquad (2)$$

and

$$\frac{\beta F_{\rm exc}}{A} = \frac{1}{2d}\sum \int_0^d {\rm d}y_1\,\rho_i(y_1)\int_\Omega {\rm d}y_2\,\rho_j(y_2) d^{ij}_{\rm exc}(y_{12}), \qquad (3)$$

with $i,j = 1,2$ in the case of one kind of particles and $i,j = 1,2,3,4$ for a heterochiral mixture. In these equations $\rho_i(y)$ is the local density of the conformation i, d is the smectic period, $d^{ij}_{\rm exc}$ is the excluded distance which is related with the excluded area through $A^{ij}_{\rm exc} = \int {\rm d}y_{12} d^{ij}_{\rm exc}$. The case of the N-Sm* phase transition for a system of one component has been already done[17]. In this work the N-Sm* and N-SmR transitions for a system of two components (heterochiral system) are developed.

First, an estimate of the free energy of a heterochiral smectic phase (SmR) is done. In a perfect aligned nematic phase, the local densities do not depend on the position and are identical, i.e. $\rho_{1,2,3,4}(y) = \rho/4$. Besides $A^{ii}_{\rm exc} = A^{jj}_{\rm exc}$, $A^{ij}_{\rm exc} = A^{ji}_{\rm exc}$, $A^{12}_{\rm exc} = A^{34}_{\rm exc}$, $A^{13}_{\rm exc} = A^{24}_{\rm exc}$ and $A^{14}_{\rm exc} = A^{23}_{\rm exc}$ (see Fig. 6 a). Therefore, the nematic free energy is then,

$$\frac{\beta F_{\rm N}}{A} = \rho\ln\rho - \rho - \rho\ln 4 + \frac{1}{8}\rho^2(A^{11}_{\rm exc} + A^{12}_{\rm exc} + A^{13}_{\rm exc} + A^{14}_{\rm exc}). \qquad (4)$$

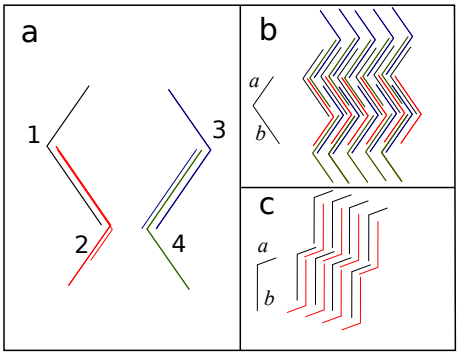

Fig. 6 (Color online) a) Representation of the considered conformations, b) self assembly in the particles for the obtained heterochiral smectic structure and c) representation of the self assembly in a homochiral smectic structure.

From the snapshots of the simulation (see Fig. 2 c) , the particles assembly for the SmR is such that each layer of the smectic phase is formed by either conformations 1 and 4 or 2 and 3 as it is sketched in Fig. 6 b. The periodicity of the layers can be modeled in the weakly ordered smectic phase by means of the first order Fourier representation of the local densities given by $\rho_{1,4}(y) = \frac{\rho}{4}(1+\varepsilon\cos(qy))$ and $\rho_{2,3}(y) = \frac{\rho}{4}(1+\varepsilon\cos(qy-\phi^*))$, where $q = \frac{2\pi}{d}$ is the smectic wave number and ϕ^* is the phase shift and ε is a parameter which goes to zero in the nematic limit. After substitution of these density dependences the ideal and excess part of the free energy become,

$$\frac{\beta F_{\rm id}}{A} = \rho\ln\rho - \rho\ln 4 - \rho + \frac{\rho}{4}\varepsilon^2, \qquad (5)$$

and,

$$\frac{\beta F_{\rm exc}}{A} = \frac{1}{8}\rho^2\sum_{j=1}^{4} A^{1j}_{\rm exc} + \left[\frac{\rho^2}{32}\left((F_{11}+F_{14})\left(1+\cos^2\phi^*\right) + 2(F_{12}+F_{13})(\cos\phi^*)\right)\right]\varepsilon^2, \qquad (6)$$

where $F_{ij} = \int {\rm d}y_{12} d^{ij}_{\rm exc}(y_{12})\cos(qy_{12})$. Therefore the heterochiral smectic free energy can be written as

$$\frac{\beta F_{\rm SmR}}{A} = \frac{\beta F_{\rm N}}{A} + \left[\frac{\rho}{4} + \frac{\rho^2}{32}\left((F_{11}+F_{14})\left(1+\cos^2\phi^*\right) + 2(F_{12}+F_{13})(\cos\phi^*)\right)\right]\varepsilon^2, \qquad (7)$$

The parameters ϕ^* and q are such that $\frac{\partial\frac{\beta F_{\rm Sm}}{A}}{\partial\phi^*} = \frac{\partial\frac{\beta F_{\rm Sm}}{A}}{\partial q} = 0$, in the first case $\phi^* = \pi$, which means that the phase is always antiferroelectric and q satisfies

$$\int {\rm d}y_{12} y_{12} d^{11}_{\rm exc}(y_{12})\sin(qy_{12}) + \int {\rm d}y_{12} y_{12} d^{14}_{\rm exc}(y_{12})\sin(qy_{12}) - \int {\rm d}y_{12} y_{12} d^{12}_{\rm exc}(y_{12})\sin(qy_{12}) - \int {\rm d}y_{12} y_{12} d^{13}_{\rm exc}(y_{12})\sin(qy_{12}) = 0. \qquad (8)$$

With the values of ϕ^* and q, it is possible to estimate the heterochiral-smectic free energy for different ε values. The coexistence density for the nematic-heterochiral smectic phase transition is given by the condition $\frac{\beta F_{\rm SmR}}{A} = \frac{\beta F_{\rm N}}{A}$, which is equivalent to the condition that the quadratic term in epsilon in Eq. 7 must vanish. From equation 9 it is obtained that $\rho_{\rm N-SmR} = \frac{4}{F_{12}+F_{13}-(F_{11}+F_{14})}$. A similar procedure was done to estimate the free energy of the homochiral smectic (Sm*) but in this case there are only two conformations such that the smectic layers are made either by conformations 1 and 2 or 3

and 4 (see Fig. 6c). As a result the free energy is,

$$\frac{\beta F_{\mathrm{Sm}}}{A} = \rho \ln \rho - \rho - \rho \ln 2 + \frac{\rho^2}{4}(A_{\mathrm{exc}}^{11} + A_{\mathrm{exc}}^{12}) + \left[\frac{\rho}{4} + \frac{\rho^2}{8}(F_{11} - F_{12})\right]\varepsilon^2, \quad (9)$$

but the equation for q is now,

$$\int \mathrm{d}y_{12}\, y_{12}\, d_{\mathrm{exc}}^{11}(y_{12}) \sin(q y_{12}) + \int \mathrm{d}y_{12}\, y_{12}\, d_{\mathrm{exc}}^{14}(y_{12}) \sin(q y_{12}) = 0, \quad (10)$$

which means that, although both smectics have an antiferroelectric order, they have different values of the smectic period q.

By equating 7 with the smectic free energy of a homochiral system (segregated case) it is possible to obtain an approximation of the densities for which such phases coexist and the intervals in which a given smectic (racemic or segregated) is more favorable as shown in Fig. 7.

The theoretical estimations of the density for which chiral segregation is reached, ρ_c^*, are given in Fig. 8 for some values of the parameter a. For $a \leq 0.2$ it is obtained that the heterochiral nematic phase is more favorable than the heterochiral and homochiral smectic phases at intermediate densities, while for densities larger than ρ_c^* the homochiral smectic becomes more favorable. For $a \geq 0.25$ the heterochiral smectic phase is the more favorable phase for intermediate densities, and for higher densities the homochiral smectic phase is again more favorable, which is in agreement with the simulations results. Although the theory underestimates the N-Sm* and SmR-Sm coexistence densities it captures the qualitative behavior obtained by the simulations.

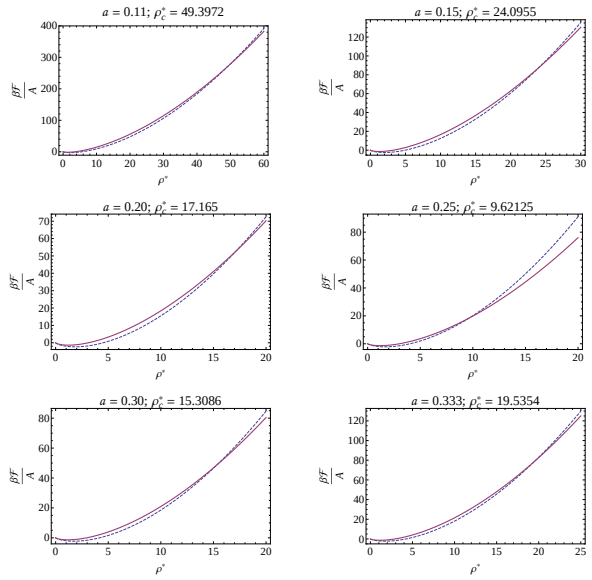

Fig. 7 Free energies for $\theta = \pi/2$ and $\varepsilon = 1$, a similar behavior is obtained for $\pi/4$. The dashed lines represent the free energy for a heterochiral phase (nematic for $a \leq 0.20$ and SmR for $a \geq 0.25$) while the continuous line corresponds to a homochiral smectic phase. On the top of each graphic we can see the corresponding parameter a and the heterochiral to homochiral smectic coexistence density ρ_c^*.

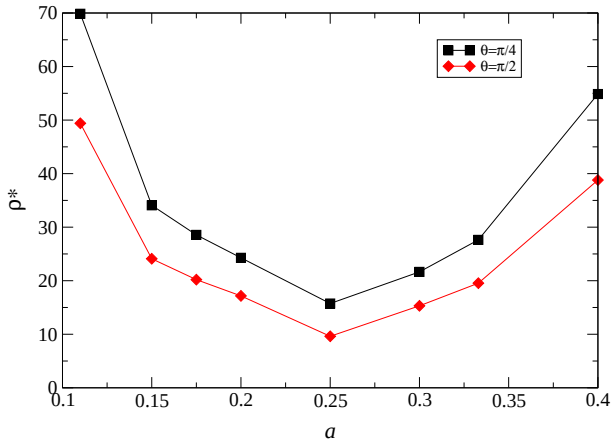

Fig. 8 Theoretical results for ρ_c^* as a function of the molecular parameter a.

4 Conclusions

An oversimplified version of the HSM made of 2-segment lines interacting with an infinitely hard potential and geometrically chiral in 2D, is capable to produce chiral segregation and several liquid crystalline mesophases. As in many other cases, chiral segregation requires high density regimes and therefore molecular ordering is achieved. For lower densities, the system exhibits different heterochiral liquid crystalline phases. This is, depending on the value of the parameter a, as density decreases the model shows nematic or smectic structures. As expected, for small values of a, close to the hard needle limit, the nematic is preferred while for large values of a, the smectic phase is generated; both heterochiral. For the lowest densities considered, the heterochiral isotropic phase is present. These features are common to both values of the molecular angle θ studied $\theta = \pi/2$ and $\pi/4$. To complement the Monte Carlo

simulation results, the second virial Onsager theory was used to predict some of the phase transitions provided by simulations, in particular, N-Sm*, N-SmR, SmR-Sm. To the best of our knowledge this is the firs time when this kind of theory is used to study chiral separation. This has been possible in this particle model, since chiral separation occures along smectic correlations.

It should be considered that the transition to the smectic phase (racemic or not) was done in the limit of parallel particles (perfect nematic) and it is useful for the study of the N-Sm phase transition. This approximation was used for the whole range of the parameter *a* even though for some regions where the phases involved (from MC) were either I or T. Despite this approximation is rough, it is interesting to notice that the qualitative behavior is captured. On the other hand, the estimation of the SmR-Sm coexistence density was done by equating the free energies of both mesophases up to the second virial approximation and using the first order Fourier representation of the local densities. Although the coexistence densities are just approximations, the development of the theory was useful to find the parameters where the found smectic mesophases are more favourable. The extension of the theory to include the isotropic-tetratic phase transition is also possible and it is part of a future work.

5 Acknowledgments

This research was financially funded by CONACYT grant 168001 and UNAM-DGAPA-PAPIIT. J.A. Martinez-Gonzalez and R. Pablo-Pedro are grateful for the support given by the CONACYT grant 168001; Julio C. Armas-Pérez is thankful to CONACYT for the Postdoctoral Fellowship No. 203840. We also gratefully acknowledge Martha Elena Buschbeck Alvarado for improving the English manuscript.

References

1 J. Jacques, A. Collet and S. H. Wilen, *Enantiomers, Racemates and Resolutions*, John Wiley & Sons, New York, 1981.
2 I. Paci, I. Szleifer and M. A. Ratner, *J. Am. Chem. Soc.*, 2007, **12**, 3545–3555.
3 N. Richardson, *Nature Materials*, 2006, **5**, 91–92.
4 P. Nassoy, M. Goldmann, O. Bouloussa and F. Rondelez, *Phys. Rev. Lett.*, 1995, **75**, 457–460.
5 R. Viswanathan, J. Zasadzinski and D. Schwartz, *Nature*, 1994, **368**, 440–443.
6 T. Huang, Z. Hu, A. Zhao, H. Wang, B. Wang, J. Yang and J. G. Hou, *J. Am. Chem. Soc.*, 2007, **129**, 3857–3862.
7 D. A. Huckaby, M. Ausloos and P. Clippe, *J. Chem. Phys.*, 1985, **82**, 5140–5145.
8 D. A. Huckaby, M. Shinmi, M. Ausloos and P. Clippe, *J. Chem. Phys.*, 1986, **84**, 5090–5094.
9 D. Andelman and P. G. de Gennes, *C. R. Acad. Sci. Paris*, 1988, **307**, 233–237.
10 I. Medved, A. Trnik, A. K. Belkasri and D. A. Huckaby, *J. Chem. Phys.*, 2007, **126**, 154512.
11 I. Paci, *J. Phys. Chem. C*, 2010, **114**, 19425–19432.
12 P. Szabelski and D. S. Sholl, *J. Chem. Phys.*, 2007, **126**, 144709.
13 R. A. Perusquia, J. Peon and J. Quintana, *Physica A*, 2005, **345**, 130–142.
14 J. Peon, J. Saucedo-Zugazagoitia, F. Pucheta-Mendez, R. A. Perusquia, G. Sutmann and J. Quintana-H, *J. Chem. Phys.*, 2006, **125**, 104908.
15 L. Onsager, *Ann. N.Y. Acad. Sci.*, 1949, **51**, 627–659.
16 S. Varga, P. Gurin, J. Armas-Pérez and J. Quintana-H, *J. Chem. Phys.*, 2009, **131**, 184901.
17 J. Martínez-González, S. Varga, P. Gurin and J. Quintana-H, *J. Mol. Liq.*, 2013, **185**, 26–31.
18 F. D. and S. B., *Understanding Molecular Simulation: From Algorithms to Applications*, Academic Press, San Diego, 2nd edn, 2002.
19 L. Gonzalez-Lee, J. Armas, J. Peon and J. Quintana, *Physica A*, 2008, **387**, 145–158.
20 J. A. Martínez-González, S. Varga, P. Gurin and J. Quintana-H, *Europhysics Letters*, 2012, **97**, 26004.
21 A. Donev, J. Burton, F. H. Stillinger and S. Torquato, *Phys. Rev. B*, 2006, **73**, 054109.
22 D. A. Triplett and K. A. Fichthorn, *Phys. Rev. E*, 2008, **77**, 011707.
23 D. Frenkel and R. Eppenga, *Phys. Rev. A*, 1985, **31**, 1776–1787.